

MECHANISM OF CONVECTIVE DRYING OF SOLUTIONS OF
FISH HYDROLYZATES IN A FOAMED STATE

A. A. Buinov, A. S. Ginzburg, and
V. I. Syroedov

UDC 664.95:547.965.047

The results of experimental investigations of the kinetics of foam drying of fish hydrolyzates are presented. The dehydration mechanism is analyzed and the enhancement of the process with dehydration of solutions in a foamed state is explained.

For the investigations, we used hydrolyzates of Caspian sprats, obtained using A. P. Chernogortsev's procedure [1]. The duration of autoprolysis, in this case, was six hours and foam generators and stabilizers were not used. The investigations were carried out on the experimental setup in [2] with different methods of energy input. It was established that the best results are obtained with convective energy input and an optimum initial solution concentration of 45-50% dry weight.

A characteristic of the process of convective foam drying is the close relation between phenomena related to the parameters and stability of the foam structure, heat and moisture transfer within and through the framework of the drying foam, the thermodynamic parameters of the bound water, and mass transfer in the boundary layer.

The nature of the drying curves of thin (0.25 mm) and thick (2.5 mm) foam layers with different air parameters (Figs. 1 and 2) indicates the complex mechanism of dehydration.

The temperature curves (Fig. 2), measured at the center of thick foam layers, are biconvex and, in addition, there is no period of time in which the temperature is constant. This indicates the low thermal conductivity of the foam layer and the complex mechanism of transport of dissolved substances and moisture within the foam. It is characteristic that the first inflection point of the temperature curves occurs at $W^c = 60-70\%$, where the intensity of moisture removal begins to decrease. The transport of heat and mass in the foam layer is affected by the motion of the pellicular fluid to the evaporation surface and the velocity of this motion depends on the temperature and thickness of the air boundary layer.

At $W^c = 60-70\%$, removal of moisture bound to the material by thermal effects begins, the nature of the drying and temperature curves changes, and the temperature of the material sharply approaches the temperature of the heating air. This indicates the presence of two drying periods: removal of moisture from the solution ($W^c \geq 60-70\%$) with relatively mobile macromolecules of the hydrolyzates and moisture bound to the material by thermal effects ($W^c \leq 60-70\%$); here, the macromolecules lose their mobility. This treatment agrees well with the classification of moisture in hydrolyzates [3] and data from a thermodynamic analysis [4].

Figure 3 shows the curves of the drying rate calculated by the method of tabular differentiation. It is evident that the rate of drying of thin foam layers is much higher than the rate of drying of thick foam layers. For low air velocities (1 m/sec), the increase in air temperature causes an increase in the drying rate; in addition, the increase in the rate of growth of the drying rate with increasing temperature is explained by the presence of pellicular fluid flow due to an increase in the gradient of the disjoining pressure in the near-surface layer of the foam structure. The motion of the pellicular fluid in the presence of a temperature gradient is a determining factor in choosing the method of energy input and explains the reasons for the rapid destruction of the foam with conductive and radiative energy inputs [2].

Astrakhan Technical Institute of Fish Industry and Management, Moscow Technical Institute of Food Industry. Translated from *Inzhenerno-Fizicheskii Zhurnal*, Vol. 43, No. 1, pp. 95-100, July, 1982. Original article submitted April 13, 1981.

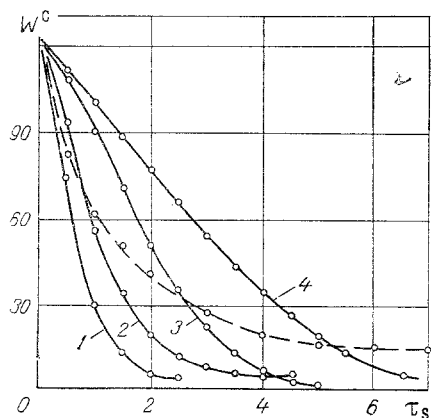


Fig. 1

Fig. 1. Drying curves of a thin (0.25 mm) foam layer (the dashed curve corresponds to drying of a solution in an unfoamed state with $V = 10$ m/sec, $t_w = 110^\circ\text{C}$): 1) $V = 10$ m/sec, $t_w = 110^\circ\text{C}$; 2) 10 and 65; 3) 1 and 110; 4) 1 and 65. W^c , %; τ_s , min.

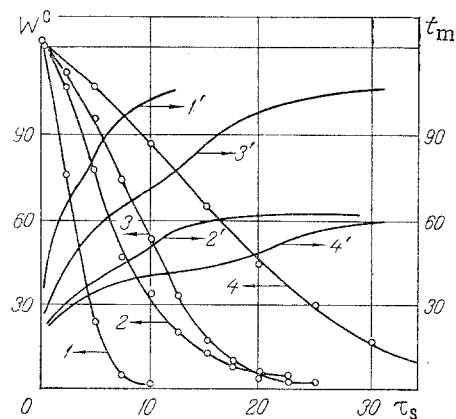


Fig. 2

Fig. 2. Drying curves (1-4) and temperature curves (1'-4') in a thick (2.5 mm) foam layer: 1-1') $V = 10$ m/sec, $t_w = 110^\circ\text{C}$; 2-2') 10 and 65; 3-3') 1 and 110; 4-4') 1 and 65. t_m , $^\circ\text{C}$.

An increase in the air velocity under identical temperature conditions increases the intensity of moisture evaporation. This in its turn enhances the flow of fluid to the surface of evaporation from the central layers of the foam, whose temperature is lower. The flow of this fluid slows down the rate of heating of the evaporation surface and the intensity of evaporation sharply increases up to $W^c = 60-70\%$ (curves 3, 7 in Fig. 3). An increase in the air velocity and temperature increases the rate of heating of the surface layer, so that in curves 5 and 8 (Fig. 3), dehydration up to $W^c = 60-70\%$ occurs at an almost constant drying rate.

The maximum values of the drying rate constitute $W^c = 60-70\%$. For lower W^c , the rate of drying sharply decreases, due to the change in the form in which the moisture is bound to the material and the endothermal effect [3], and the nature of the motion of moisture inside the material also changes.

With $W^c < 60-70\%$, the distance between the macromolecules of the hydrolyzate decreases. Since the mobility of water molecules is higher than that of the macromolecules of the hydrolyzate, the moving moisture in this case can be viewed as a flow of water films between flexible hydrolyzate macromolecules. As is well known [5], the motion of water films is due to the disjoining pressure gradient. Since the removal of pellicular moisture is related to the presence of an endothermal effect, an increase in the temperature of the material increases the rate of drying, the process is limited by the external heat transfer conditions, and an increase in the air temperature plays a basic role. For curves 2, 3 and 6, 7 in Fig. 3, it is evident that during the period of decreasing rate of drying, it is more advantageous to increase the temperature of the air than its velocity.

According to the classification of A. V. Lykov [5], the curves of the rate of drying in the second period correspond to the fifth type. The rate of drying at first decreases along a curve that is convex with respect to the abscissa axis. This means that the intensity of pellicular moisture transfer decreases more rapidly than the intensity of moisture exchange due to an increase in the binding energy. The inflection point indicates, evidently, a change in the mechanism of internal moisture transfer and the coordinates of this point are more precisely determined from the temperature curve ($W^c \approx 30\%$, Fig. 2). This agrees well with data from a thermodynamic analysis [4] (vanishing of the temperature gradient coefficient).

With further decrease in W^c (Fig. 3), the thickness of the fluid films decreases, a process which is due to the considerable flexibility of the macromolecules of the hydrolyzate, and the film space transforms into molecular microcapillaries. Mass transfer in this case is determined by the effusion of water molecules through the microcapillaries.

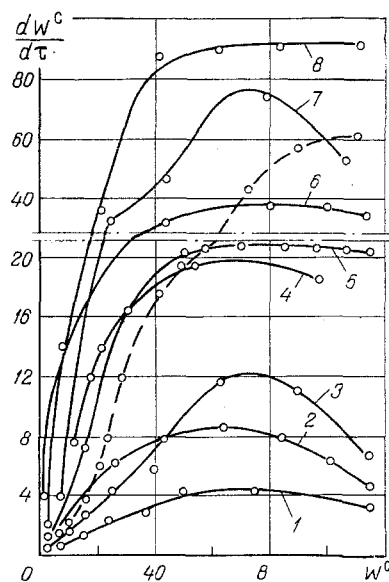


Fig. 3. Curves of the rate of foam drying (1-4 are for a foam layer of 2.5 mm and 5-8 are for a foam layer of 0.25 mm): 1) $V=1$ m/sec, $t_w=65^\circ\text{C}$; 2) 1 and 110; 3) 10 and 65; 4) 10 and 110; 5) 1 and 65; 6) 1 and 110; 7) 10 and 65; 8) 10 and 110 (the dashed curve shows the rate of drying of an unfoamed solution with $V=10$ m/sec, $t_w=110^\circ\text{C}$). $dW^c/d\tau$, %/min.

In order to estimate the effect of foam formation on drying with film and effusive moisture transfer, a layer of foam (0.25 mm) was deposited on the base [2], the foam was destabilized, and at the same time a thin even layer of fluid was formed. The drying process was conducted at comparable air temperature (110°C) and air velocity (10 m/sec).

Figure 1 shows the drying curve of an unfoamed solution (dashed line), on whose basis the drying rate curve was constructed (Fig. 3, dashed line). According to the classification of A. V. Lykov [5], the drying rate curve of unfoamed hydrolyzates belongs to the rarely encountered sixth type. Drying occurs at all times during the period in which the rate decreases, and in this case, the rate of decrease in the drying rate sharply changes with $W^c \approx 60\%$. Since the thermal conductivity of the fluid is higher than that of the foam layer, the drop in the drying rate to $W^c = 60\%$ (in comparison with curve 8) is explained by increased entropic binding of the moisture in the solution. With $W^c < 60\%$, there is a significant settling of the near-surface layer and the gradient in the disjoining pressure that arises creates a flow of moisture from the inner layers toward the surface, but the rate of decrease of this flow depends on the thermal conductivity of the fluid and the amount of pellicular moisture per unit of evaporation surface. In foam drying, volume evaporation is observed inside the

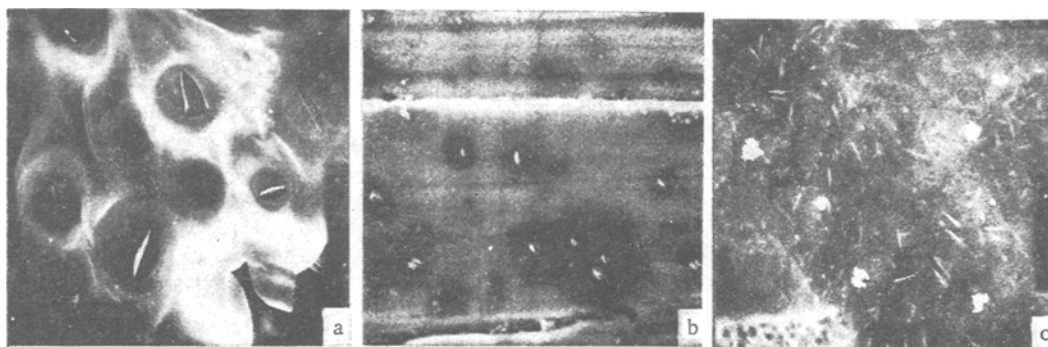


Fig. 4. Electron microphotographs of the dried solution of hydrolyzate.

foam framework and due to the extended internal surface, the rate of foam drying with pellicular internal moisture transfer is much higher.

With $W^c \approx 30\%$, the drying rate curve of the unfoamed solution has an inflection point, which also indicates a change in the internal moisture transfer mechanism. The evaporation zone enters deeper into the material and effusive moisture transfer occurs. Since the magnitude of the effusive flow is determined by the integrated area of the microcapillary openings and by the number of microcapillaries per unit area of evaporation surface, in the presence of volume vaporization in the foam structure, the magnitude of the integral effusive flux will be greater than in the unfoamed solution and the rate of drying will also be higher (curve 8, Fig. 3).

Thus, the significant enhancement with foam drying compared to drying in an unfoamed state is explained by the extended internal surface of the foam structure and the presence of volume vaporization.

In the surface foam bubble layer, after the moisture in the solution is removed, the pellicular moisture is removed through the external foam surface. As a result of intense thermal action, the flow of vapor into a bubble can exceed the flow of vapor through the external film and, as a result, the pressure in the bubble increases sharply, its diameter increases, and if the film is not strong enough, the bubbles break.

Figure 4a shows a typical electron microphotograph ($\times 1000$) of the upper section of the foam, in which rupture of bubbles is clearly seen. The rupture edges are bent back, which indicates the fact that the rupture occurred at a stage of high elasticity of the films.

Microphotography of the foam layers established that the average diameter of foam bubbles increases during the drying process. The diameter of bubbles in the upper layer increases insignificantly with an increase in the thickness of the foam layer. The dimensions of the bubbles in the foam layer next to the bottom increase sharply with increasing thickness of the foam layer, which supports the conclusion as to the mechanism for the stability of the foam structure during the drying process.

Figure 4b shows an electron microphotograph of a section of an unfoamed solution dried on a metallic base ($\times 6000$). Here, the dark sections with high density of matter are clearly evident; the small sections have a circular shape and the large sections are formed from several small sections. Apparently, these are hypomolecular formations, associates of macromolecules of the hydrolyzate, whose presence in solutions with high concentrations affected the anomalies in the viscous and foam-forming properties [6]. The dimensions of the associates were estimated in the range 1.5–3.0 μm .

It is characteristic that at the center of the associates there is a light dot — a pore having an average diameter of 0.1 μm . The basic reason for the formation of such pores is the increase in the magnitude of the disjoining pressure, which is a function of the intermolecular interaction. The presence of such pores at the center of an associate confirms the assumption that at a certain moisture content, pellicular moisture transfer occurs under the action of the disjoining pressure gradient.

Figure 4c shows electron microphotographs of a dried layer of unfoamed solution with a thickness of about 0.3 mm ($\times 1000$). Here, quite large pores with an equivalent diameter of about $(3-4) \cdot 10^{-4}$ cm are visible. The pores have uneven edges, which suggests that nonrelaxing stresses inside the material, due to the significant settling of the surface layers occurring while the material acquires sufficient rigidity during the drying process, are the basic reason for their formation.

During drying in the foamed state, pores at the center of the associates and pores due to settling of layers help in the diffusion transfer of vapor through the foam framework into the air.

NOTATION

Here W^c is the moisture content of the material relative to the mass of dry matter, %; τ_S , duration of the dehydration process, min; $dW^c/d\tau$, rate of dehydration, %/min; V , air velocity above the foam layer, m/s; t_w , air temperature above the foam layer, $^{\circ}\text{C}$; t_m , temperature of the material, $^{\circ}\text{C}$.

LITERATURE CITED

1. A. P. Chernogortsev, Small Fish Processing Based on Fermentation of the Stock [in Russian], Pishchevaya promyshlennost', Moscow (1973).
2. A. A. Buinov and A. P. Chernogortsev, "Problem of drying fish protein hydrolyzates," Tr./KTIRPKh (1978), No. 76; Technological Processes and Equipment for Fish Processing Enterprises in the Western Basin, pp. 3-7.
3. A. A. Buinov, A. S. Ginzburg, and V. I. Syroedov, "Hygroscopic properties of fish protein hydrolyzates dried in a foamed state," Izv. Vyssh. Uchebn. Zaved., Pishchevaya Tekhnol., No. 3, 110-113 (1977).
4. A. A. Buinov, "Thermodynamic analysis of the mechanism of interaction of food fish hydrolyzates with water," Tr./MTIPP (1977), Progress in the Technology of Drying Different Products and Materials, pp. 86-89.
5. A. V. Lykov, Theory of Drying [in Russian], Energiya, Moscow (1968).
6. A. A. Buinov, A. S. Ginzburg, and V. I. Syroedov, "Effect of depth of fermentation on the properties of fish food hydrolyzate foams," Izv. Vyssh. Uchebn. Zaved., Pishchevaya Tekhnol., No. 1, 132-134 (1978).

TEMPERATURE FIELD OF GRAPHITE ELECTRODE IN PLASMATRON

N. V. Pashatskii, E. A. Molchanov, and
S. A. Chugin

UDC 533.924

Results of an experimental study are presented pertaining to the temperature field of a graphite electrode in an ac power plasmatron.

Graphite electrodes have found broad applications, in electrometallurgy and electric welding, in light sources, in plasmatrons, and in many other devices. The electrodes in such devices operate at high current densities and under heavy heat loads, at temperatures near their melting point. A study of the temperature field of such an electrode is of both scientific and practical interest, inasmuch as indeed the temperature determines many processes occurring in the electrode body and at the electrode surface (electron emission, heat conduction, radiation, erosion of material, etc.).

Most attention in the technical literature on this subject has been paid to the thermal state of carbon and tungsten electrodes with a small diameter [1-3]. The surface temperature is measured most effectively by methods of optical pyrometry [2, 3]. In this way have been determined temperature distributions over the radius of the end face and over the length of the lateral surface of an electrode, also the dependence of the electrode bulk temperature on the current and on the length of the electrode rod. In another study [4] the temperature field of a thick (diameter $d \sim 0.5$ m) graphite electrode was measured by the thermoelectric method.

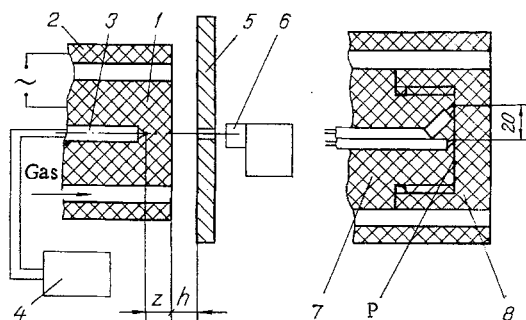


Fig. 1. Schematic diagram of experimental apparatus: 1) rod-type electrode, 2) graphite sleeve, 3) thermocouple, 4) model KSP4 potentiometer, 5) fusible wall, 6) model OPPIR-017E pyrometer, 7) electrode body, 8) front assembly.